Aalborg Universitet

On the Stability and Performance of Remote DOE Laser Cutting

Villumsen, Sigurd; Kristiansen, Morten; Olsen, Flemming Ove

9th International Conference on Photonic Technologies - LANE 2016

On the stability and performance of remote DOE laser cutting

Sigurd Lazic Villumsen[a,*], Morten Kristiansen[a], Flemming O. Olsen[b]

a Aalborg University, Aalborg 9220, Denmark
b IPU, Kgs. Lyngby 2800, Denmark

Abstract

When considering remote laser cutting, the literature often discusses two methods: remote fusion cutting (RFC) and remote ablation cutting. It has previously been hypothesised that remote cutting can be conducted by modifying the intensity profile of the laser beam by means of a diffractive optical element. In this study, the effect of travel speed, focus offset and angle of incidence on the stability of remote cutting with a customized beam pattern was investigated. The study is based on a set of remote cutting experiments conducted on a 3kW single mode fiber laser in 0.5 mm stainless steel. The study showed that remote cutting is obtainable with speeds ranging from 800mm/min-1600mm/min by using an average laser power of 630 W. Furthermore, the experimental results showed that the cutting stability remained high for a larger range of incident angles.

© 2016 The Authors. Published by Elsevier B.V. This is an open access article under the CC BY-NC-ND license
(http://creativecommons.org/licenses/by-nc-nd/4.0/).
Peer-review under responsibility of the Bayerisches Laserzentrum GmbH

Keywords: Beam-shaping; laser cutting; remote laser cutting; diffractive optical element

1. Introduction

Recent advances in the field of high quality high-intensity lasers have spurred increased industrial interest in remote laser cutting (RLC). The remote position of the cutting head in RLC means that the laser beam can be moved over the workpiece by angling the cutting head, or by angling the scanner mirrors in the case of scanner cutting heads (Zaeh et al. (2010) and Lu et al (2013)). This can potentially lead to faster cutting rates as scanner systems are capable of moving the beam over the workpiece at speeds exceeding 900m/min. The remote position of the cutting head furthermore reduces the risk of cutting head workpiece collisions. However, the drawback of this

---

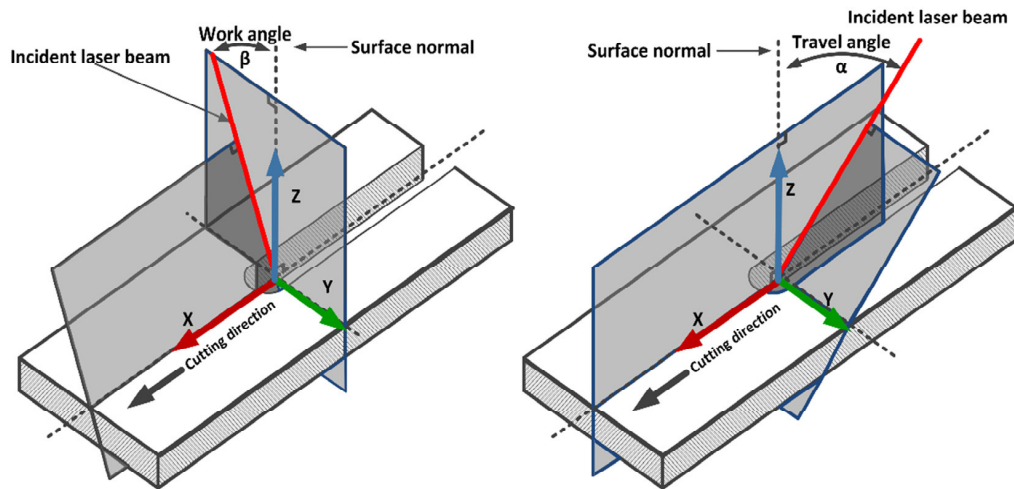* Corresponding author. Tel.: +45-30130852 .
 E-mail address: sv@m-tech.aau.dk

Fig. 1. The decomposition of the angle of incidence used in this paper. The angle is decomposed into definition of the work angle β and the travel angle α. The arrow indicates the cutting direction.

type of beam movement is that it changes the angle of incidence of the beam on the workpiece. As the stability of the cut can be affected by the angle of incidence, it is necessary to identify the extent to which the beam can be moved by angling the cutting head for remote cutting processes.

In remote fusion cutting (RFC), a cut is achieved by finding cutting parameters where laser induced pressure phenomena eject the molten material from the cutting kerf, see for example Matti et al (2013). The cut is achieved with one exposure of the beam, whereas in remote ablation cutting the beam needs to be scanned over the workpiece repeatedly. However, the RFC process is sometimes described as unstable for certain materials and parameters (Pihlava et al (2013)). In considering the stability of RFC related to changes in the incident angle, Villumsen et al (2015) have shown that, with a 3kW single mode fiber laser setup, stable cuts could only be obtained for $\pm 6°$. To increase the repeatability of the process more knowledge of how the melt ejection is obtained is necessary. Currently, modelling of the laser process is being used as a way to improve this knowledge (Zaeh et al (2013)).

In Olsen et al (2009 and 2011) it is discussed that the melt flow in the kerf can be manipulated by changing the beam intensity profile. By selecting an appropriate intensity pattern the melt ejection of remote and gas- assisted cutting can be improved. Improving the melt ejection can increase the cut quality and possibly the travel speed. The task of determining an appropriate intensity pattern is however challenging as there is an infinite number of possible designs. Furthermore the size of the shaped beam is larger than the raw laser beam. If not accounted for in the optical setup this leads to more material being melted and, as a consequence, slower cutting rates (Villumsen et al (2014)). Nonetheless, the approach has been used successfully for both laser cutting and welding. Kaakkunen et al (2014) show that by dividing the beam into multiple spots, it is possible to enhance the cutting quality and decrease the cutting gas pressure required for gas-assisted laser cutting. Victor et al (2011) show that in high-power (10kW) fiber laser welding, the weld toe angle can be improved by shaping the laser using a diffractive optical element (DOE). Hansen et al (2014) show that by applying beam shaping through the use of a DOE, it is possible to increase control over the size and depth of the weld pool for laser welding.

This paper investigates the stability of remote laser cutting with a customized beam intensity pattern obtained by using a DOE inserted in the beam path. The investigation describes how the travel speed, focus offset and angle of incidence affects the stability of the resulting remote DOE cutting process. Furthermore this is compared to another single pass remote laser cutting process - RFC.

This paper is organized as follows. In Section 2, the definitions and methodology are introduced. This includes descriptions of the angular decomposition, the stability measure, and the experimental setup and experimental procedure. In Section 3, the results of the experiments are presented and compared with the earlier results obtained for RFC presented in Villumsen et al (2015). In Section 4, some concluding remarks are presented.

2. Definitions and Methodology

In the following, a definition of stability is presented, along with a definition of the angular representation. Subsequently, the experimental procedure is described, as are the DOE pattern and cutting parameters.

2.1. Definition of angular representation

In this paper, the angle of incidence of the laser beam is represented by a work and travel angle as described in Villumsen et al (2015). This decomposition can be seen from Fig 1, where the travel angle is denoted α and the work angle β. Fig 1 shows that both α and β are defined as the angular deviation from the normal vector of the surface of the work piece.

2.2. Definition of the measure of stability

To achieve a quantitative measure, cut stability is defined on the basis of the ability of the cutting process to eject molten material from the cutting kerf, as described in Villumsen et al (2015). This means that stable sections are characterized by an unblocked cutting kerf and unstable sections by a blocked cutting kerf. If the total length of the cutting kerf is denoted l_C and the total length of the stable regions is denoted l_S, then the total stability S of a cut can be evaluated as a percentage, as in equation (1).

$$S = \frac{l_S}{l_C} \cdot 100\% \tag{1}$$

In small sections, the cutting kerf can become partially unblocked, due, for example, to turbulence in the melt. To ensure that these small sections are removed, a minimum stability length of l_{min} is introduced. If an unblocked section shorter than l_{min} is found, it is removed and treated as unstable. By tuning the distance l_{min}, it is possible to filter out spurious holes in the kerf while still ensuring that small stable sections are taken into account. If this definition is used, the stability of a cut can be evaluated purely by investigating its cutting kerf. This ensures that all stability evaluations can be conducted by visual inspection without the need to monitor the cutting process itself.

2.3. Evaluation of stability

To ensure a uniform way of assessing the cutting stability for a set of experiments an automated stability evaluation was used. The first step in the stability evaluation was to capture images of the entire cutting kerf on all samples. This was done using a programmable Carl Zeiss Axio imager microscope with an x2.5 objective. An example of the resulting cutting kerf images of a cut can be seen in Fig. 2. These images were then exported to Matlab, in which an image stitching algorithm had been implemented. By using this image stitching algorithm the images seen in Fig. 2 were concatenated into one large image. This can be seen in Fig. 3. To analyze the cut stability, a computer vision based algorithm was implemented in Matlab, giving two results: first, a stability measure, defined as a percentage of the cut with an unblocked cutting kerf, and second, the stitched image with a color overlay showing areas of stability and instability. Fig. 4 shows the resulting overlay obtained from the analysis of Fig. 3. A more through description of the system is given in Villumsen et al (2015).
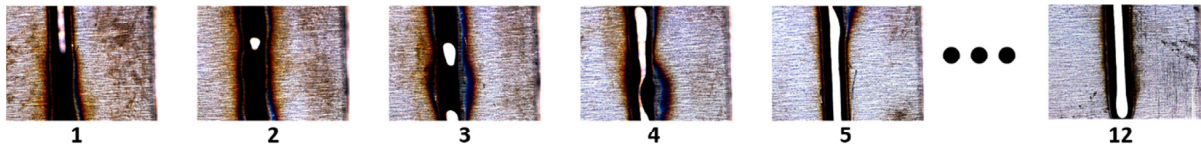
Fig. 2. A set of images captured by the programmable microscope. A total of 12 images was necessary to obtain images of the entire kerf. The first and the last were removed to ensure that only images of the cutting kerfs were present.
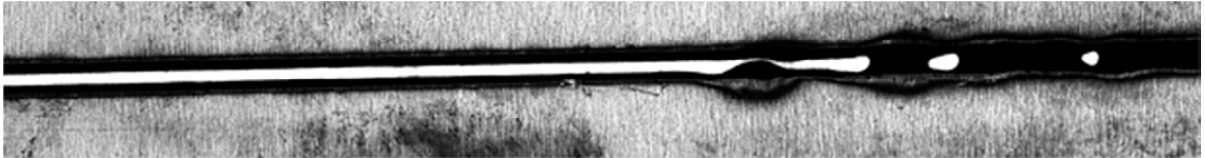

Fig. 3. The resulting stitched image obtained from the individual images seen in Fig. 2. The resulting image has been converted to grayscale to reduce the computational load in the subsequent steps.
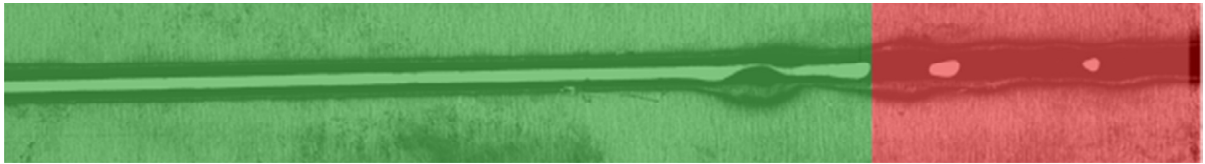

Fig. 4. The stitched image seen in Fig. 3 with an applied overlay of color describing the areas of stability (green) and the areas of instability (red). The overlay was used purely for manual inspection. The output used was the stability measure described in section 2.2.

2.4. Experimental procedure

Two sets of experiments were conducted to evaluate the stability of the remote DOE cutting process. Both experimental series were conducted as parameter studies. The first experimental series investigated how travel speed and focus offset affected the stability of the cutting process. On the basis of the results of these experiments, the parameters yielding the most stable cuts were used for the second set of experiments. The second set of experiments investigated how the work and travel angle affected the stability of the cut. This experimental structure can be seen in Fig. 5.

These two sets of experiments used the experimental setup illustrated in Fig. 6. A cutting head was mounted on an industrial robot. The cutting head contained the traditional optical components, such as a collimating lens, a focusing lens and cover slides. To obtain the customized intensity profile a diffractive optical element was inserted in the collimated beam in the cutting head.
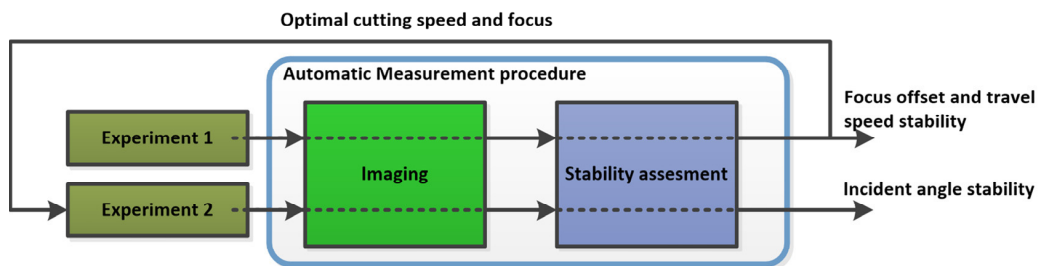

Fig. 5. The experimental procedure presented in this paper. Two sets of experiments were conducted. In the first set, the stability of the remote cutting proces was evaluated as a function of the travel speed and focus offset. In the second set of experiments, the stability was evaluated as a function of the incident angle of the laser beam. The results were obtained by an automatic measurement system.
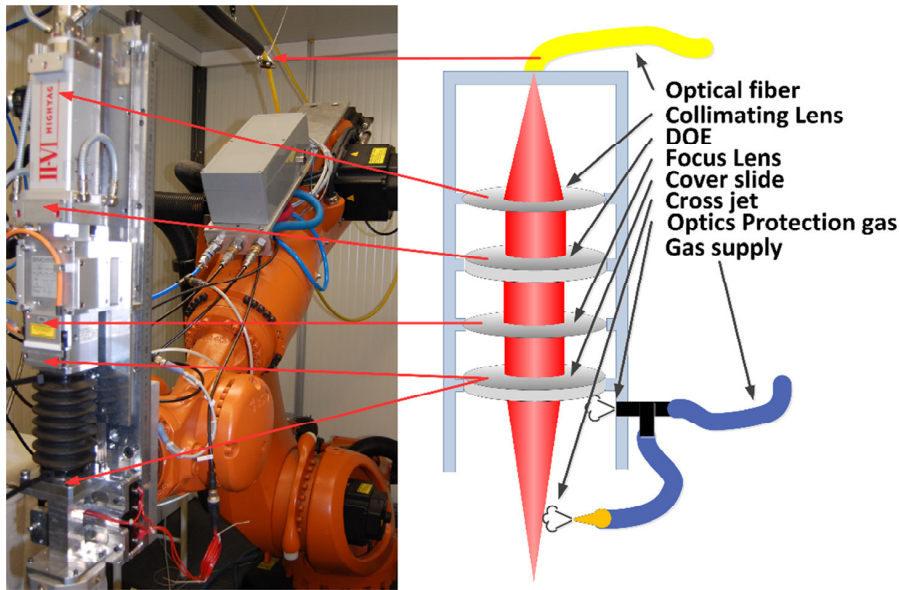
Fig. 6. The experimental setup used in the experiments. The diffractive optical element (DOE) was inserted in the collimated beam path. Furthermore, it should be noted that compressed air was only used for protecting the optics and not as a cutting gas.

To prevent dust and ejected molten material from entering the cutting head, compressed air was applied. Furthermore a cross jet was applied for further protection. It should be noted that compressed air was only applied for protection purposes and not as a cutting gas. In all experiments, the movements were conducted with an XY table situated underneath the cutting head. Table 1 provides a summary of the equipment and common cutting parameters used in all experiments.

Table 1. Equipment and common cutting parameters. It should be noted that the mode of operation of the laser was pulsed.

Equipment	Type and manufacturer	Parameter	Value
Industrial robot	KUKA Quantec kr120 R2500	Power	3kW
Laser	3kW IPG YLS-3000 (Single mode)	Material	SST EN Type:X2CrNi19-11 No. 1.4307
Cutting head	HighYag 470mm focal length	Thickness	0.5mm
XY positioning system	Q-sys	Cutting gas pressure	0 Bar (Air cross jet)
		Laser mode of operation	Pulsed (21% duty cycle)

As the table indicates, the mode of operation of the laser was pulsed. The duty cycle was 21%, which means that the laser was emitting an average power of 630W.

2.5. Beam pattern

As discussed in the introduction to this paper and in Section 2.4, a diffractive optical element (DOE) was inserted into the cutting head after the collimating lens. The DOE was manufactured by the company II-VI from zinc sulfide, processed by diamond turning. By inserting the DOE into the beam path the approximately Gaussian intensity profile depicted on Fig. 7 was transformed into the distribution seen on Fig. 8. Both intensity profiles were captured by the measurement equipment described in Hansen et al (2013). The cutting direction of the pattern shown in Fig. 8 was upwards.
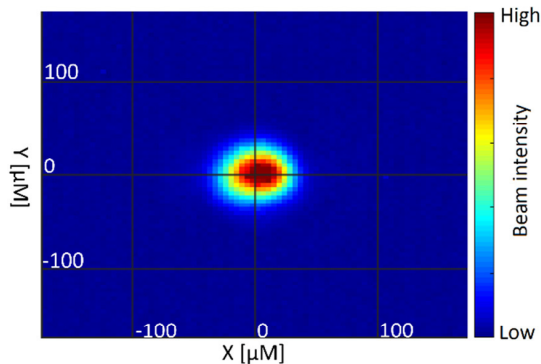
Fig. 7. The intensity profile of the unmodified beam of the IPG YLS-3000 single mode fiber laser. The image was captured in the beam waist.
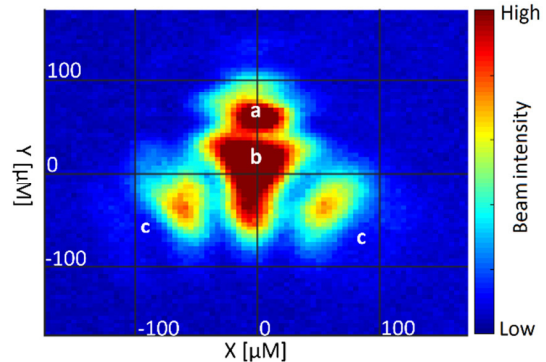

Fig. 8. The intensity profile of the modified beam when passed through the DOE. The image is captured +7 mm away from the beam waist.

The idea behind the use of beam patterns for remote cutting originates from the knowledge of the melt flow in traditional keyhole laser cutting and welding. Here the dominant direction of the melt flow is horizontal around the laser beam (Preissig et al (1994)). In remote fusion cutting this horizontal flow is combined with a downwards motion of the melt due to the vapor pressure in the processing area (Schober et al 2012). This essentially means that melt flow in laser cutting and welding can be guided by applying melt guiding laser irradiation in the cutting kerf. By choosing an appropriate intensity distribution a more efficient melt ejection can be obtained. The energy distribution presented in Fig. 8 is a refinement of the work presented in Olsen et al (2009 and 2011) and Villumsen et al (2014).

The width of the pattern can be seen to be approximately 200 μm. Pihlava et al (2013) have reported that the cutting kerf for RFC exceeds 600 μm in a MM fiber laser setup. However, for RFC conducted with single mode fiber lasers narrower kerfs have been reported. In Kristiansen et al (2015) it is reported that cutting kerf widths ranging from 179-363 μm were obtained. The experimental setup used were identical to the one presented here, except for the presence of the DOE. This means that the pattern size approximately equals the cutting kerf width for RFC on a SM fiber laser.

The shape of the intensity distribution shown in Fig. 8 originates from an iterative design process in which several beam designs have been investigated. The shape is composed of three main components, a melt beam **a**, a lid beam **b** and two trailing beams **c.** The melt beam forms a keyhole around which the material flows. The lid beam induces a vapor pressure that forces the molten material downwards. The trailing beams are used for further guiding the melt and cut edge trimming. The pattern shown in Fig. 8 shows the beam +7mm away from the beam waist as cuts have been obtained in this focus area and as the three beam components **a-c** are easier to separate here.

2.6. Experiment 1: Effects of beam diameter and travel speed on process stability

As Fig. 5 indicates, experiment 1 investigated the effect of focus offset variations and travel speed on the stability of the remote DOE cutting process. This was achieved by means of a parameter study in which α and β were kept constant at $0°$. The focus offset was adjusted by moving the cutting head 1mm at a time. The travel speed was changed by adjusting the G-code program used for programming the XY positioning system. This is summarized in Table 2.

Table 2. Table describing the process variables for experiment 1. Items marked by [a] indicate that the minimum value was found by a set of preliminary experiments not presented in this paper and that experiments were stopped when no stable cuts were obtained.

	Travel speed[a]	Focus offset[a]	Work angle	Travel Angle	Repetitions	Number of cuts
Experiment 1	800-1800 mm/min steps of 200 mm/min	0 - +10 mm in steps of 1mm	$0°$	$0°$	3	198

The focus offset used in the above table was defined as the distance from the beam waist of the beam pattern to the top of the sheet. Preliminary experiments indicated that only positive focus offsets (beam waist above workpiece surface) was of interest with regards to cutting.

2.7. Experiment 2: Effects of travel and work angle on process stability

The goal of the second experiments was to determine the effect of the work and travel angle on remote DOE cutting stability. The work and travel angle was adjusted using the industrial robot. By defining a robot tool calibration from the robot TCP to the beam waist (The minimum diameter of the beam pattern), it was possible to adjust the work and travel angle by means of the robot teach pendant without changing the focus offset. The experimental parameters used for the second experiment are summarized in Table 3.

Table 3. Table describing the process parameters for the second experiment. Items marked [a] were found from the first set of experiments. The marking [b] indicates that experiments were stopped when no stable cuts were obtained.

	Travel speed[a]	Focus offset[a]	Work angle[b]	Travel Angle[b]	Repetitions	Number of cuts
Experiment 2	1200 mm/min	+5 mm	0-34° in steps of 2°	0-16° in steps of 2°	6	1026

3. Results

As discussed in the description of the experimental procedure in section 2.1, two sets of experiments were conducted. One involved finding a parameter window for travel speed and focus offset within which the remote cutting process could be achieved, and one involved the task of finding a parameter window for the travel and work angle.

3.1. Results from experiment 1

To find an appropriate stability window for travel speed and focus offset, several experiments were conducted with travel speeds ranging from 800 mm/min to 1600 mm/min and with focus offset ranging from 0 to +10 mm. The focus offset was adjusted in steps of 1 mm and the travel speed in steps of 200 mm/min. Figs. 9 and 10 were created by applying the automatic stability measurement system. Fig. 9 shows the minimum stability obtained in the three
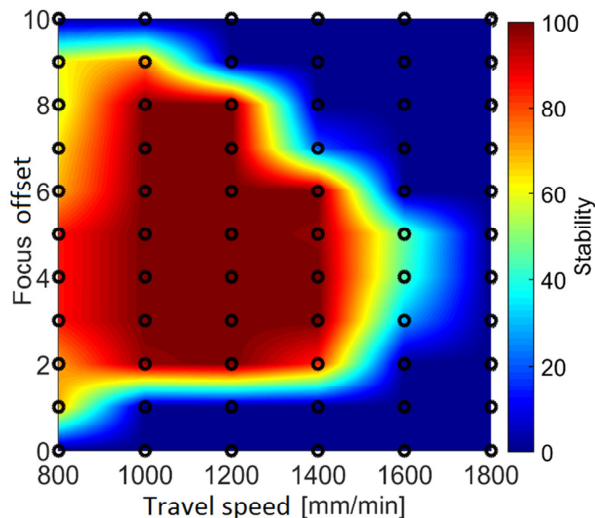

Fig. 9. The resulting minimum stability measures obtained in the 3 repetitions of the first experiment. Notice the large stable region in the center of the stable region, where stability measures of 100% were obtained for all repetitions.
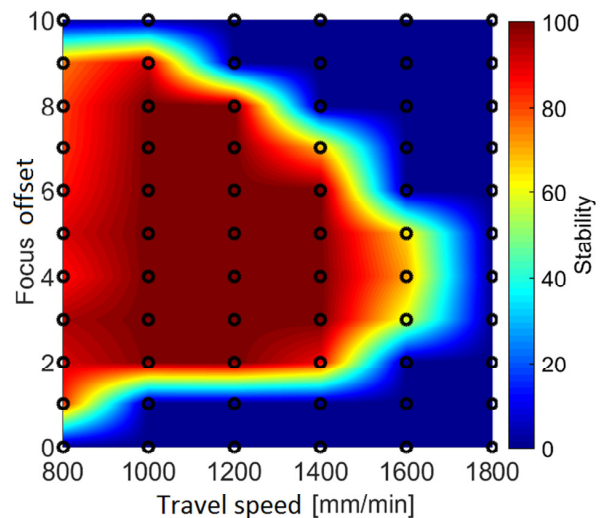
Fig. 10. The resulting average stability measures obtained for the 3 repetitions of the first experiment. Notice that the region of stability is coherent and only degrades towards the extremes of the parameter space.
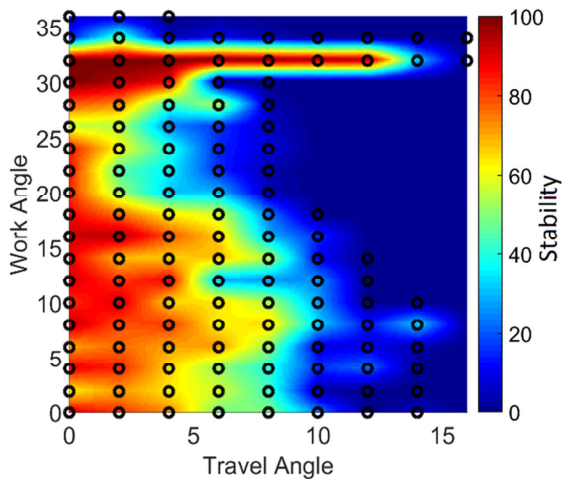
Fig. 11. The resulting average stability of experiment 2, where the work and travel angle are varied and the stability of the process is evaluated.
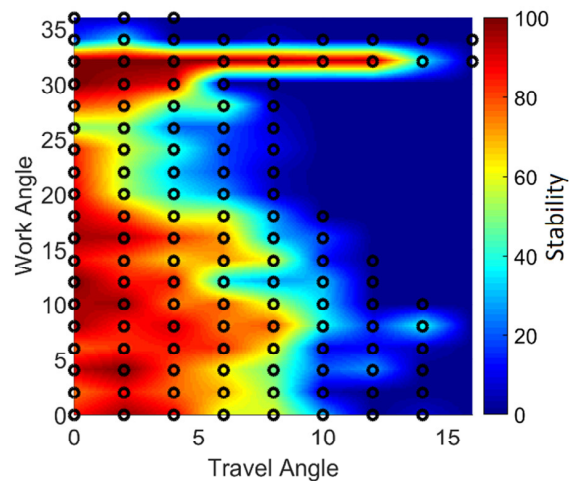
Fig. 12. The resulting average stability of experiment 2 when the first experiment from each plate has been removed.

repetitions of remote DOE cutting. It should be noted that the black dots on the figures indicate actual measurements and the colored overlay represents linear interpolation between these measurement points. Fig. 10 shows the average stability of the cutting process for the three repetitions. As this figure shows, the stability of the cuts rose to 100% in a large part of the process window.

It can be seen from Fig. 9 that most cuts conducted with a travel speed between 1000 and 1400 mm/min were 100% stable, which means that all repetitions were completely cut through. The resulting region of stability is coherent without any decline in its central part. As discussed in section 2.4, the travel speed and focus offset parameters yielding the highest stability should be used for the subsequent experimental series. On the basis of the results displayed in Fig 9 and Fig. 10, the decision was made to perform experiment 2 with a travel speed of 1200 mm/min and with a focus offset of 5 mm.

3.2. Results of experiment 2

The second experiment investigated the effect of the incident angle of the beam on process stability. The results of this experiment can be seen from Fig. 11 and Fig. 12. Fig. 11 shows the process stability as a function of the work and travel angle. From this figure it is seen that the stability of the process decreased when passing travel angles of 4-5° with cuts being obtainable with travel angles of 8°. When considering work angle the declination was however much less pronounced. As Fig. 11 shows, cuts were obtained with a work angle of as much as 32° when using the beam pattern. It should be noted that an interesting outlier is located close to the work angle cutting limit in Fig. 11. For a work angle equal to 32°, a line of 100% stability can be observed. The area of 100 % stability can be seen for 8 travel angle measurements (0° −14°) with 6 repetitions. In other words, it is quite unlikely that they originated from statistical fluctuations. One could argue that the non-round beam used in this paper creates a very complex melt flow around the generated keyholes. Furthermore, the pulsed mode of operation used in these experiments could induce and amplify the natural melt oscillations in the kerf caused by the angular dependency of the absorbed intensity as described in Olsen (2011-2). This could indicate that unexpected areas with good melt ejection characteristics could arise in areas where these coupled effects interact with each other beneficially. However, a cause for the outlier has not been found and it disappears when a work angle of 34° is reached. Further research could investigate this unexpected 'sweet spot' to see if a 32° projection of the cutting beam pattern could entail better cut stability. Also, it could be investigated if changing processing parameters such as duty cycle changes the position and size of this area.
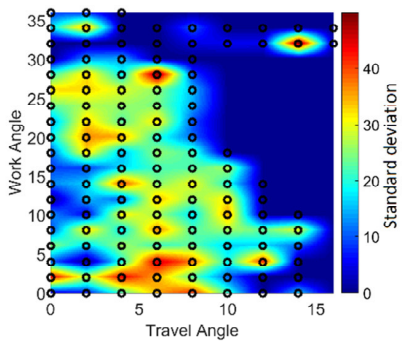
Fig. 13. The standard deviation of the cuts when all 6 repetitions are included.
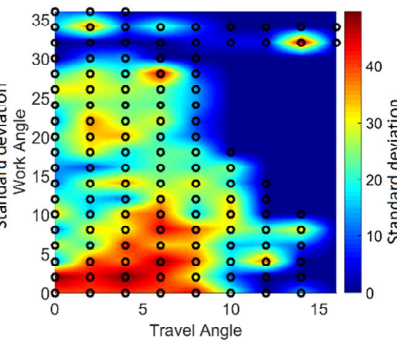
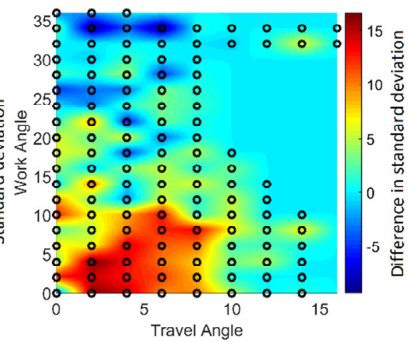Fig. 14. The standard deviation of the cuts when the first cut is removed.

Fig. 15. The difference in standard deviation between Fig. 13 and Fig 14.

During the course of this experimental investigation, there was a slight tendency for the first cut in the 6 repetitions to perform slightly differently with regards to stability than the subsequent experiments. To investigate this, the standard deviations of each data point were calculated for all 6 repetitions and compared to the standard deviation of the last 5 repetitions to determine if the first experiment introduced a larger variance in the data. These two plots can be seen in Figs 13 and 14, and the difference between them is presented in Fig. 15. From Fig. 15, it can be seen that the difference is most pronounced in the low angle regions, where the presence of the first sample increases the variance. It is assumed that this is caused by thermal lensing in the diffractive optical element. To correct the obtained results in Fig. 11 the stability value of the first repetition is removed and the average stability value is recalculated. The results from these recalculations can be seen from Fig 12. The resulting plot shows higher stability in the low angle regions as indicated by Figs. 13 -15.

3.3. Comparing experiment 1 to RFC results

In Villumsen et al (2015) it is investigated how the travel speed, focus offset and angle of incidence affects the stability of the RFC. As all experiments were conducted on the same experimental setup used in this paper, except for the presence of the DOE, a direct comparison between remote DOE cutting and RFC can be made. Fig. 16 shows combined stability plot for the two processes. It has two areas of stability: one from RFC and one from remote DOE cutting. From this figure it can be seen that the level of stability for cuts obtained with remote DOE cutting is generally higher than the stability achieved with RFC. Furthermore, the area of stability is much more coherent. However, the increase in stability comes at the cost of travelling speed, which is approximately 20% of the travelling speed of RFC cuts. It should be noted that RFC cuts were unobtainable for slower speeds than 5000mm/min. Villumsen et al (2015) determined the limit for remote fusion cutting (RFC) to be $\pm 6°$ when using the full 3kW laser power. However, the overall stability level for RFC was much lower and $\pm 6°$ was seen as the limit to where cuts were possible. For remote DOE cutting it was discussed that the stability decreased when passing travel angles of 4-5° with cuts being obtainable with travel angles of 8°. The difference between the stability of the two processes much more pronounced when it comes to the work angle. Villumsen et al (2015) determined that the work angle limitation for RFC was identical to the travel angle limit. For Remote DOE cutting, cuts were obtained with a work angle of as much as 32°.

Furthermore, it was in Villumsen et al (2015) noted that the repeatability of their RFC experiments were very low with the chosen equipment. This tendency was not observed for remote DOE cutting. Finally it should be noted that the remote DOE cuts presented in this paper were all conducted with an average power of 630 W. In contrast, RFC required the full 3kW CW beam.
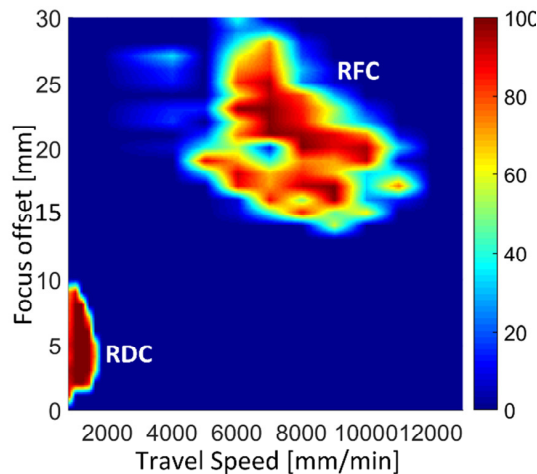
4. Concluding remarks

Fig. 16. The combined stability plot of RFC and remote DOE cutting (RDC). From this plot it can be seen that the stability of remote DOE cutting has a more coherent area of stability. Furthermore, the average stability in the region is close to 100% for all parameter values.

In this paper, the stability of remote DOE cutting has been investigated by means of a set of experiments. The effect on process stability of changing the focus offset, the travel speed, and the incident angle was investigated by means of an automatic stability measurement system. It was determined that remote cuts could be conducted with travelling speeds ranging from 800mm/min-1600mm/min. Furthermore, it was determined that stable cuts could be obtained within a focus range of 8mm. In considering the effect of incident angle on the stability of the process, the angle was decomposed into a work angle and a travel angle. Stable cuts were obtained for travel angles up $8°$. When considering work angle cuts could be achieved with work angles up $32°$. When compared to remote fusion cutting (RFC) the remote DOE cuts were obtained at approximately 20% of the travel speed of RFC. The area of stability was however found to be much more coherent, with average stability measures exceeding that of RFC. Furthermore the cuts were conducted with an average power of 630W, which is much lower than the power required for RFC.

References

A. Schober, J. Musiol, R. Daub, J. Feil, M.F. Zaeh, Laser Assisted Net shape Engineering 7 (LANE 2012) Experimental Investigation of the Cutting Front Angle during Remote Fusion Cutting, Physics Procedia, Volume 39, 2012, Pages 204-212.

Hansen, K. S., Olse, F. O., Kristiansen, M., and Madsen, O. Design of measurement equipment for high power laser beam shapes. In Proceedings of The 14th Nordic Laser Materials Processing Conference NOLAMP 14 (2013).

Hansen, K., Kristiansen, M., and Olsen, F. Beam shaping to control of weldpool size in width and depth. Physics Procedia 56 (2014), 467–476.

K.-U. Preissig, D. Petring and G. Hertziger (1994), High speed laser cutting of thin metal sheets, proc. SPIE 2207,96-110.

Kaakkunen, J. J. J., Laakso, P., and Kujanpää, V. Adaptive multibeam laser cutting of thin steel sheets with fiber laser using spatial light modulator. Journal of Laser Applications 26, 3 (2014).

Kristiansen, M., Villumsen, S., and Olsen, F. O. (2015), Modelling of the remote fusion cutting process based on experiments. *Physics Procedia 78* 110 – 119. 15th Nordic Laser Materials Processing Conference, Nolamp 15.

Lu, Jinhong, and Veli Kujanpää. 2013. "Review study on remote laser welding with fiber lasers." Journal of Laser Applications 25 (5).

Matti, R. S., T. Ilar, and A. F. H. Kaplan. 2013. "Analysis of laser remote fusion cutting based on a mathematical model." Journal of Applied Physics 114 (23).

Olsen, Flemming O.(2009) Klaus Schütt Hansen, and Jakob Skov Nielsen. 2009. "Multibeam fiber laser cutting." Journal of Laser Applications (Laser Institute of America) 21 (3): 133-138.

Olsen, Flemming O.(2011). "Laser metal cutting with tailored beam patterns." Industrial Laser Solutions 17-19.

Olsen, Flemming O.(2011-2) Laser cutting from CO2-laser to disc- or fibre laser – possiblities and challenges. In ICALEO.

Pihlava, A., Purtonen, T., Salminen, A., Kujanpää, V., and Savinainen, T. Quality aspects in remote laser cutting. in: Welding in the World 57, 2

(2013), 179–187.

Pihlava, Anssi, Tuomas Purtonen, Antti Salminen, Veli Kujanpää, and Timo Savinainen. 2013. "Quality aspects in remote laser cutting." Welding in the World (Springer-Verlag) 57 (2): 179-187.

VICTOR, B., FARSON, D., REAM, S., WALTERS, C. Custom beam shaping for high-power fiber laser welding. Welding journal 90, 6 (2011).

Villumsen, S., and Kristiansen, M. (2015) Angular stability margins for the remote fusion cutting process. Physics Procedia 78, 89 – 98. 15th Nordic Laser Materials Processing Conference, Nolamp 15.

Villumsen, Sigurd, Steffen Nordahl Joergensen, and Morten Kristiansen. 2014. "Flexible Laser Metal Cutting: An Introduction to the ROBOCUT Laser Cutting Technique." 7th World Conference on Mass Customization, Personalization, and Co-Creation (MCPC 2014), 217-228. Aalborg.

Zaeh, M.F., J. Moesl, J. Musiol, and F. Oefele. 2010. "Material processing with remote technology revolution or evolution?" Physics Procedia 5, Part A (0): 19-33.